

SUPPLEMENTARY MATERIAL for Fujisawa and Barraclough

TABLE S1. Comparisons of alternative search strategies versus an exhaustive search of 100 gene trees each with four species and five individuals sampled per species

	$N_{\text{opt}}^{\text{a}}$	$N_{\text{single}}^{\text{b}}$	N^{c}
Single threshold	10	-	-
Multiple threshold + Arbitrary start	46	67	-
Multiple threshold + single threshold start	61	79	22

^a N_{opt} : Number of trials in which search reached the global optimum

^b N_{single} : Number of trials in which search found likelihood higher than ST.

^c N : Number of trials in which MT+ST found likelihood higher than MT+Arbitrary start.

SUPPLEMENTARY FIGURE LEGENDS

Figure S1. Comparison of likelihood values found by 3 search methods: single threshold (ST) against multiple threshold (MT) with multiple arbitrary starting sets (left panel) and against multiple threshold search starting from ST results (right panel). Open circles represent the likelihood of ST and MT search on a simulation trial, and solid line indicates $y=x$. Crosses show likelihood values of true optima found by exhaustive search, plotted against ST results. Trials in which crosses and dots converge were those in which the MT search reached the true optimum.

Figure S2. Boxplots of the size of the 95% confidence set for a) single threshold and b) multiple threshold versions of the method, shown for each simulation type as defined in the Methods and each effective population size. The line within each box shows the median, the box limits show the inter-quartile range, and whiskers/points indicate extreme values.

Figure S3. The estimated scaling parameters for A) the diversification branching process and B) the coalescence branching process across each combination of simulation type (B to H) and effective population size, using the multiple threshold method. The horizontal dashed line indicates a value of 1, which is expected under the default model assumed in simulation B of a constant-rate diversification process and a neutral coalescent process with no substructure and constant population sizes.

Figure S4. The accuracy of delimitation across simulations varying in the length of simulated DNA sequences. Separate plots are shown for each of the four effective population sizes used in

the simulations. Black dashed lines indicate the predicted curves for the GMYC, and grey dashed lines for the curve for the 2% distance clustering.

Figure S5. The results of delimitation of *Rivacindela* from the mitochondrial gene tree of Pons et al. (2006). Branches indicated by red lines represent species entities delimited by the ML model obtained by the single threshold GMYC. The numbers on nodes are the GMYC supports calculated with models included in 95% confidence set. Only support values > 0 are shown here.

Figure S6. The results of delimitation of *Neocicindela* from the mitochondrial gene tree of Pons et al. (2011). Branches indicated by red lines represent species entities delimited by the ML model obtained by the single threshold GMYC. The numbers on nodes are the GMYC support calculated with models included in 95% confidence set. Only support values > 0 are shown.

Figure S7. The effect of proportion of monophyletic species on the accuracy of delimitation for simulation B with the single (left) and the multiple threshold (right) method. Solid curves are responses predicted by GLM ($z=10.7$, $p<<0.001$ for the single threshold, $z=9.85$, $p << 0.01$ for the multiple threshold).

FIGURE S1

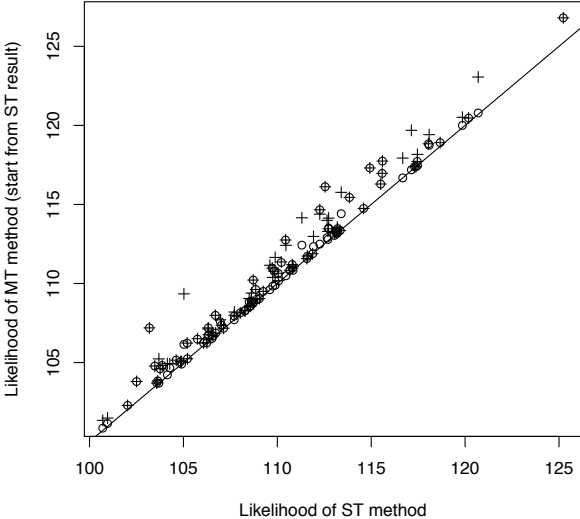
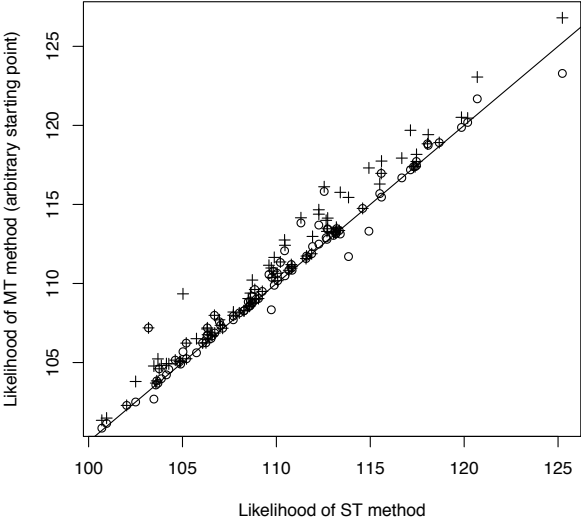
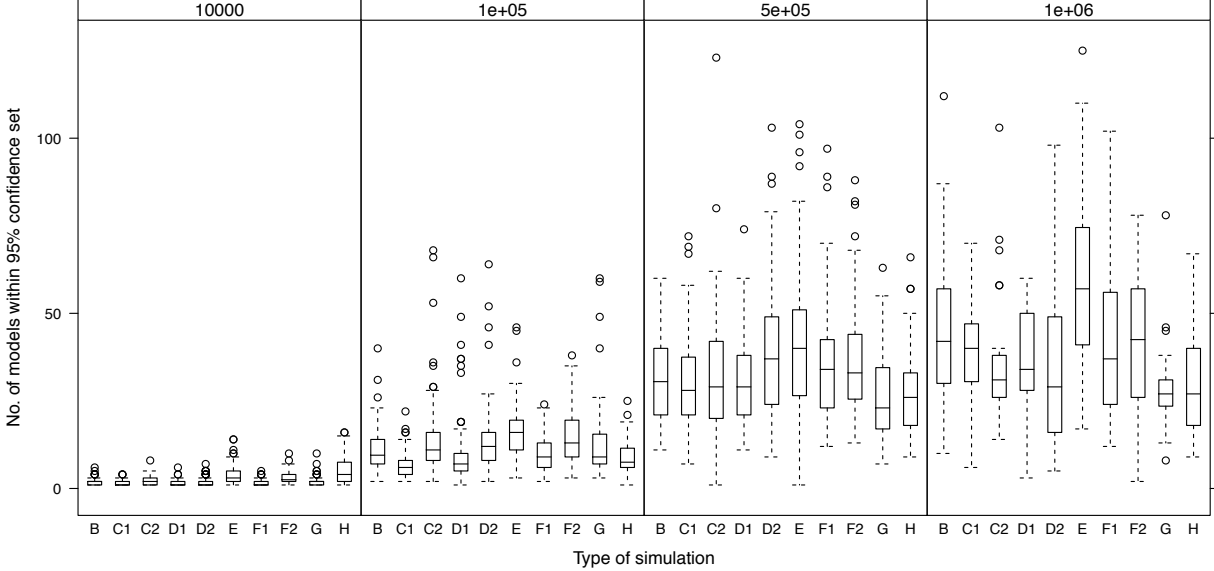


FIGURE S2

a)



b)

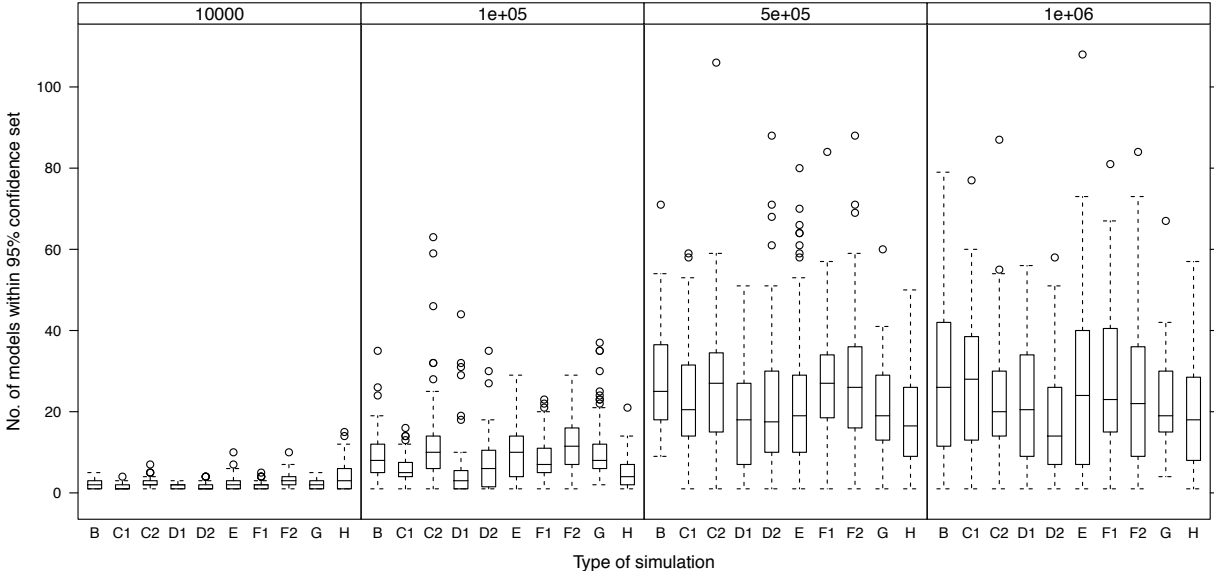
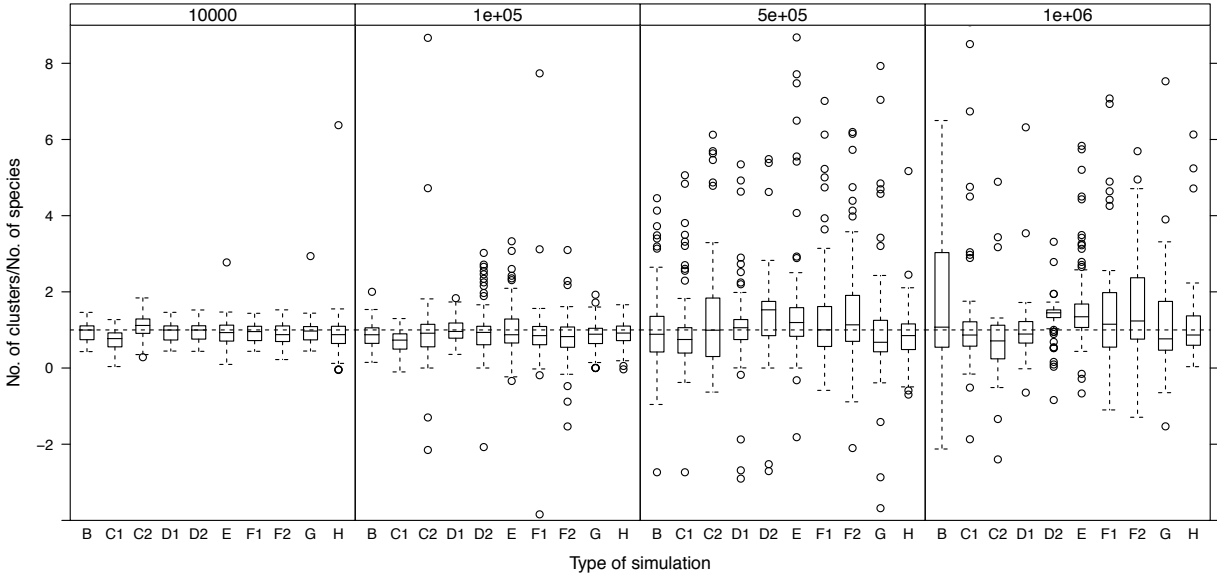


FIGURE S3

a)



b)

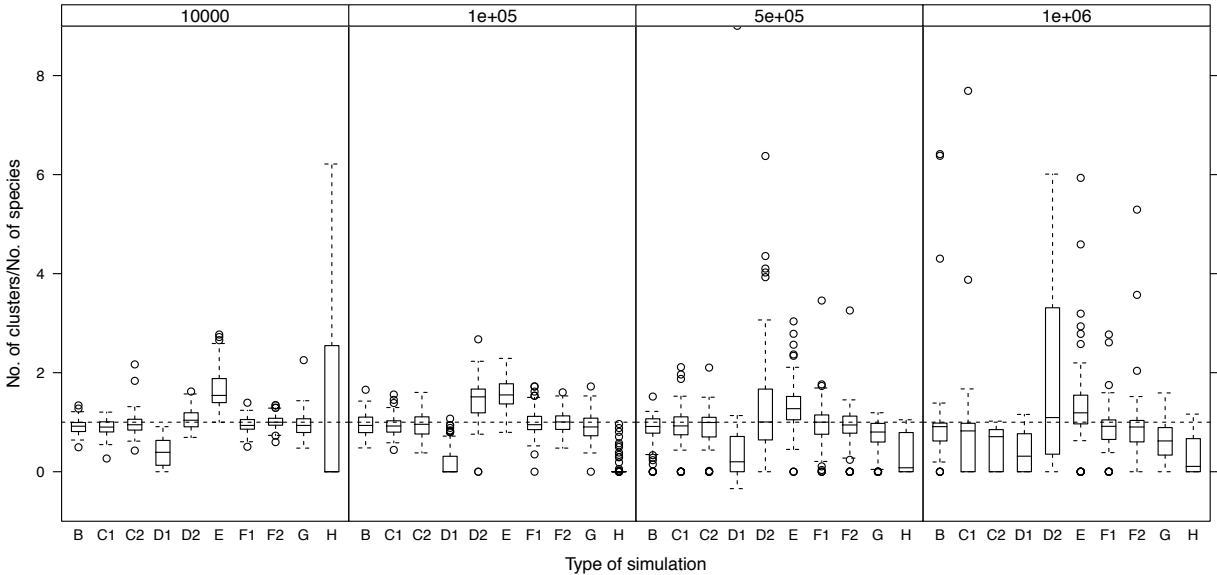


FIGURE S4

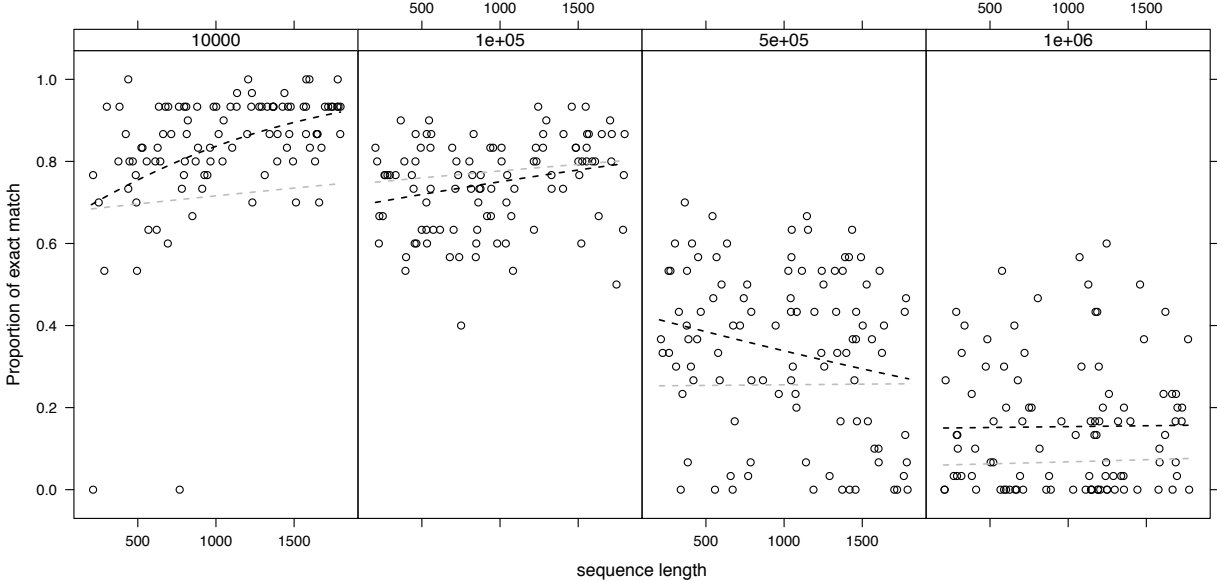


FIGURE S5

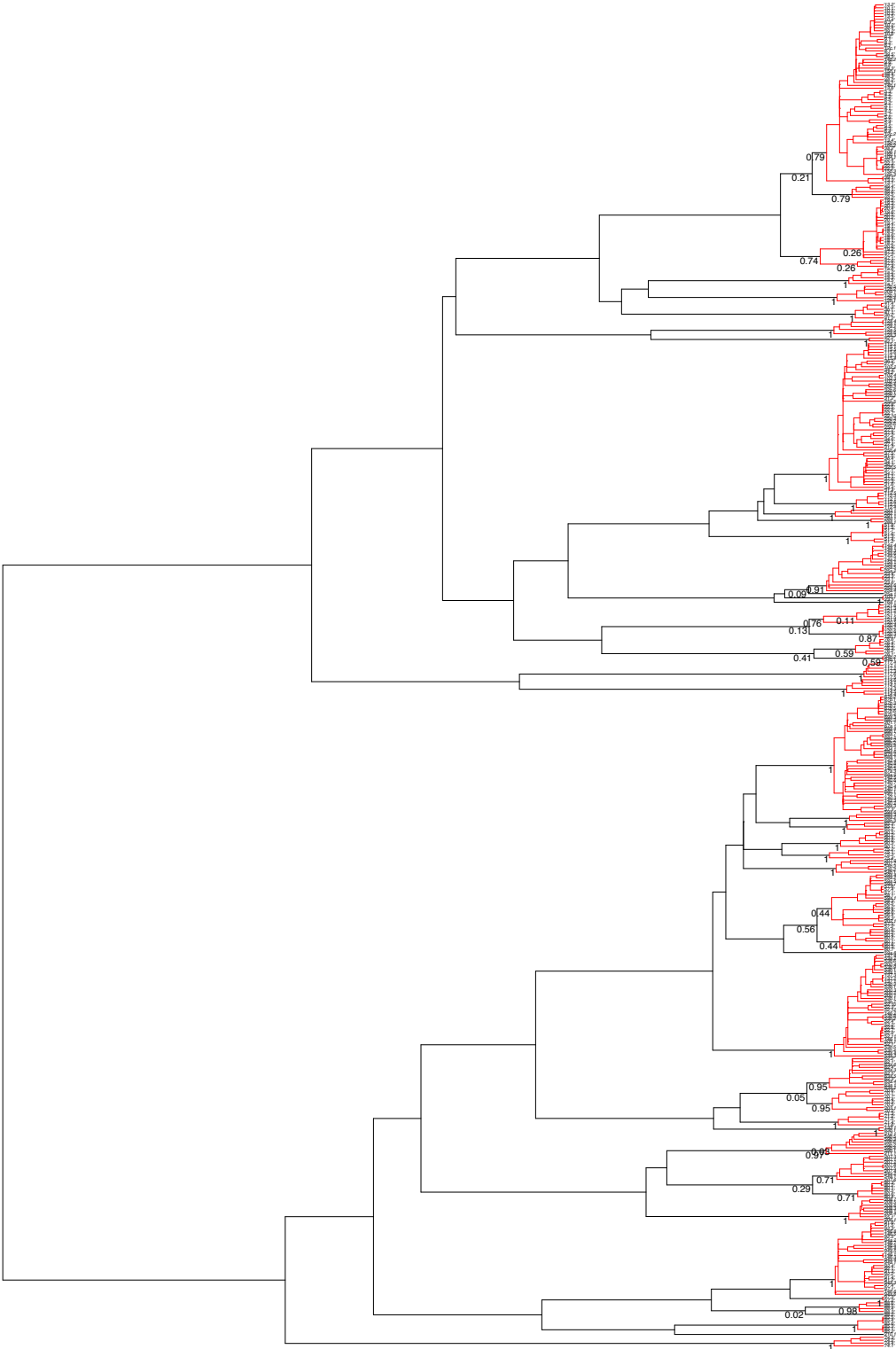


FIGURE S7

